INFLUENCE OF RESIDUAL ABERRATIONS ON THE ERROR OF A FISEAU INTERFEROMETER

V. G. Maksimov and I.G. Polovtsev

Design and Technology Institute «Optika»,
Siberian Branch of the Russian Academy of Sciences, Tomsk
Received March 27, 1996

We discuss here the influence of residual aberrations on the errors of optical elements control with a Fiseau interferometer. We proposed a technique to calculate the maximum admissible values of residual aberrations in the illuminating arm of the interferometer to meet a desirable accuracy of the interferometric measurements.

Since the quality of optical components determines the errors of various measurements, one should use high-quality optical antennas in problems of astronomy and optical sounding of the atmosphere. Monitoring of the shape of optical surfaces is an inherent part of the technology of optical components production. The most accurate device for this purpose is a laser interferometer.[8]

Figure 1 presents the optical arrangement of a Fiseau interferometer (FI). A parallel light beam from a laser source *1* is expanded in a collimator *2*, passes through a light-dividing element *3*, and is focused at the point F' by a lens *4*. The aplanatic light-dividing meniscus *5* is placed behind the lens so that its back surface has the center of curvature at the point F'. The wave front reflected from that surface is the standard reference front. After the reflection from the tested surface *6* and passing through the same way backwards (as the center of curvature of the surface *6* also coincides with the point F'), this wave front portion interferes with the reference front. The interference pattern can be recorded with a photo- or video camera *7*. The deviations from the ideal profile of the surface tested can be estimated from the observed pattern. The estimation is performed visually or by digital processing of the interferogram.[4] This scheme is rather versatile because it proposes a possibility of installing components of radius $R_{\text{c.l.}}$ which can vary within the laser coherence length.

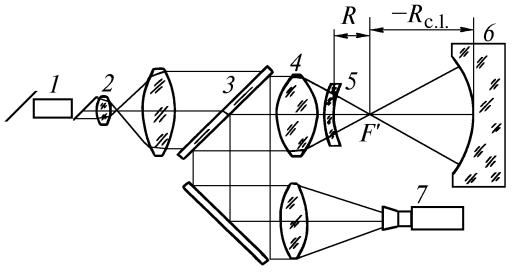

FIG. 1. Optical arrangement of the Fiseau interferometer.

The error of interference measurements in FI is influenced by the following factors:

1) errors in processing the interferograms;

2) quality of the reference surface;

3) residual aberrations of optical elements of the interferometer.

The first two factors are rather evident because they appear in the interferogram equation directly. As to the residual aberrations, the FI distinction is that there are no optical surfaces between the reference surface and the tested component. Therefore, the residual aberrations in the illuminating arm $W_{\text{r.a.}}$ must be compensated for, but not completely. The reason is the difference between the reference and objective arms $(R_{\text{r}} - R_{\text{c.l.}})$.

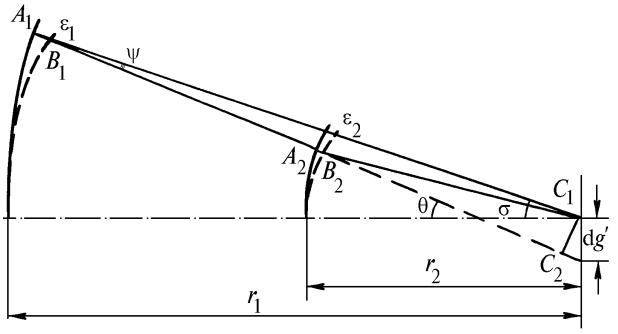

FIG. 2. Scheme of the wave front motion.

Let us consider Fig. 2 (Ref. 1). It shows the motion of the wave front from the position ε_1 to the position ε_2. By the cosine law, one can write

$$(B_2C_1)^2 = (B_1B_2)^2 + (B_1C_1)^2 - 2(B_1B_2)(B_1C_1)\cos\psi ,$$

$$B_1C_1 = r_1 - N_1 ; \quad B_2C_1 = r_2 - N_2 ;$$

$$B_1B_2 = r_1 - r_2 ; \quad \cos\psi = \left[1 - \left(\frac{\mathrm{d}g'\cos\theta}{r_1 - N_1}\right)^2\right]^{1/2}$$

where N_1 and N_2 are wave aberrations of the fronts ε_1 and ε_2 at the points B_1 and B_2 lying on one and the

0235-6880/96/08 720-05 $02.00

same ray; C_1 is the center of paraxial sphere; r_1 and r_2 are paraxial radii of curvature of wave fronts ε_1 and ε_2; dg' is the transversal geometric aberration of the ray B_1B_2.

Then, for N_2, we have

$$N_2 = r^2 - \left[(r_1 - r_2)^2 + (r_1 - N_1)^2 - 2(r_1 - r_2)(r_1 - N_1)\cos\psi\right]^{1/2}. \quad (1)$$

If the reference sphere for the front ε_2 is chosen to be not a paraxial sphere with the center of curvature at the point C_1, but a different one whose center is displaced by the distance dz with respect to the Gaussian plane, the formula (1) takes the form

$$N_2 = r_2 + dz\left(1 - \frac{\rho^2}{2}\sin\sigma\right) - [(r_1 - r_2 + dz)^2 + (r_1 - N_1)^2 - 2(r_1 - r_2 + dz)(r_1 - N_1)\cos\psi]^{1/2}, \quad (2)$$

where $\rho = \frac{(m^2 + M^2)^{1/2}}{a}$; m and M are coordinates of the point B_1 of the wave front ε_1; σ is the back aperture angle; $2a$ is the light diameter of the front ε_1.

The relations (1) and (2) demonstrate that in the general case the wave aberration of the front ε_1 changes with its propagation. The value of the change is determined by geometrical parameters r_1, r_2, $r_1 - r_2$, σ and by the initial aberration N_1. Let W_1 denote the wave aberration of the front having passed the objective arm of FI to the tested component and backwards when it meets the wave front reflected from the reference surface of the meniscus, and let W_2 be the wave aberration of the front reflected from the reference surface of the meniscus. Then the FI error $\Delta W(x, y)$ caused by the transformation of the residual aberration $W_{r.a.}$ is defined by the relation

$$\Delta W(x, y, W_{r.a}) = W_2(x, y, W_{r.a}) - W_1(x, y, W_{r.a}), \quad (3)$$

where x, y are the coordinates of a point on the reference surface of the meniscus.

The influence of $W_{r.a.}$ on ΔW was studied earlier.[5–7] In the present paper, we try to represent $\Delta W(W_{r.a.})$ in the form convenient for use in the interferometer design. The method of numerical simulation is chosen as a method of studying $\Delta W(x, y, W_{r.a.})$. The program is based on the standard algorithm for calculating the ray path through an optical system.

It is well known that the wave aberration function can be expanded into a power series at every point of the output pupil over the normalized polar coordinates of this point. The expression for it has the following form[2]:

$$W(\rho, \varphi) = \sum_i \sum_j W_{ij}\,\rho^i \cos^j\varphi$$

or

$$W(\rho, \varphi) = W_{00} + W_{20}\,\rho^2 + W_{11}\,\rho\cos\varphi + W_{40}\,\rho^4 + W_{31}\,\rho^3\cos\varphi + W_{22}\,\rho^2\cos^2\varphi + \ldots, \quad (4)$$

where W_{ij} is the coefficient of wave aberration expressed in terms of wavelengths and equal to the value of the wave aberration at the edge of the output pupil for $\rho = 1$, $\varphi = 0$; $i \geq j$; $i + j$ is an even number; $i + j - 1$ is the order of expansion; W_{00} is a constant term which does not influence the quality of a pattern (usually, it is not included in the expansion); the other summands correspond to geometrical aberrations: defocusing, transversal displacement (first order of expansion), spherical aberration, coma, astigmatism (third order of expansion), etc. The transversal aberration components involved in the relations (1) and (2) are connected with the wave aberration by the following relations[2]:

for the meridional component

$$\partial g' \cong \frac{1}{\sin\sigma}\left[\cos\varphi\,\frac{\partial W(\rho, \varphi)}{\partial\rho} - \frac{\sin\varphi}{\rho}\,\frac{\partial W(\rho, \varphi)}{\partial\varphi}\right];$$

and sagittal component

$$\partial G' \cong \frac{1}{\sin\sigma}\left[\sin\varphi\,\frac{\partial W(\rho, \varphi)}{\partial\rho} + \frac{\cos\varphi}{\rho}\,\frac{\partial W(\rho, \varphi)}{\partial\varphi}\right]. \quad (5)$$

Figure 3 presents the simulation results for spherical aberration, coma, astigmatism, and curvature of the image field. These results demonstrate that ΔW is of the same character as $W_{r.a.}$ from the viewpoint of the expansion (4); it also makes reasonable to consider only the meridional component of aberrations.

Typical dependences $\Delta W(R_r - R_{c.l.})$ are shown in Fig 4. The analysis of the dependences makes it possible to come to the following conclusions:

– spherical aberration brings the largest contribution to ΔW, other conditions being equal;

– if an optical component is installed to provide minimal bending of the interferogram fringes (plane of best adjustment), the spherical aberration is compensated for by 73.1%, coma by 57.7%, astigmatism by 50%, the curvature of the image field is compensated for completely;

– from the viewpoint of stability with respect to $W_{r.a.}$, best tested components are concave ones, while the worst components are convex ones lying within the interval

$$R_{c.l.} < R_r/5. \quad (6)$$

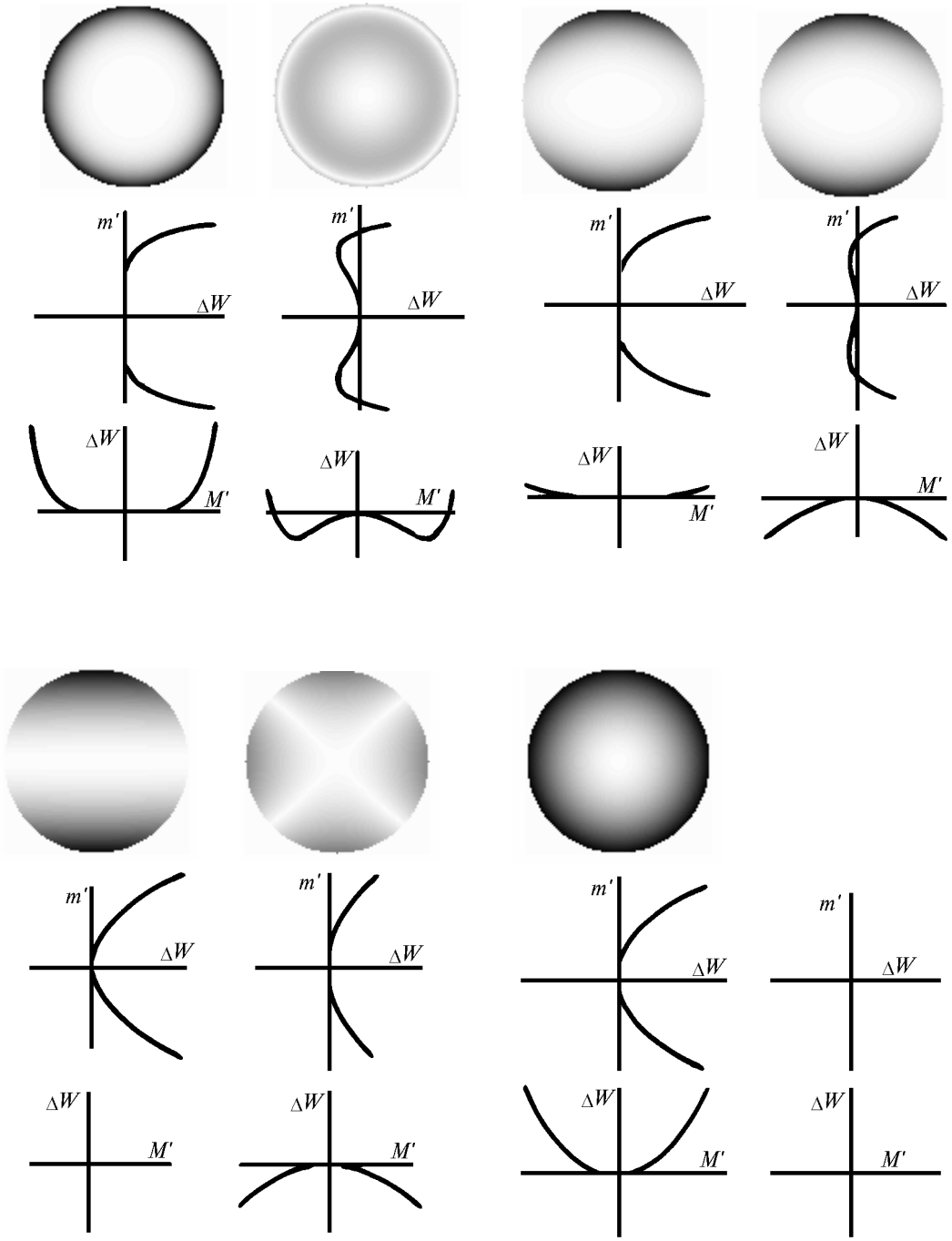

FIG. 3. Distribution of ΔW (relative units) in the plane of a lens output pupil (upper pairs of pictures) and also in meridional and sagittal sections (middle and lower pairs of pictures) under the presence of a) spherical aberrations; b) coma; c) astigmatism; d) curvature of the image field. Left and right pictures correspond to ΔW at the installation of the curvature center of the tested component in the Gaussian plane and in the plane of the best adjustment.

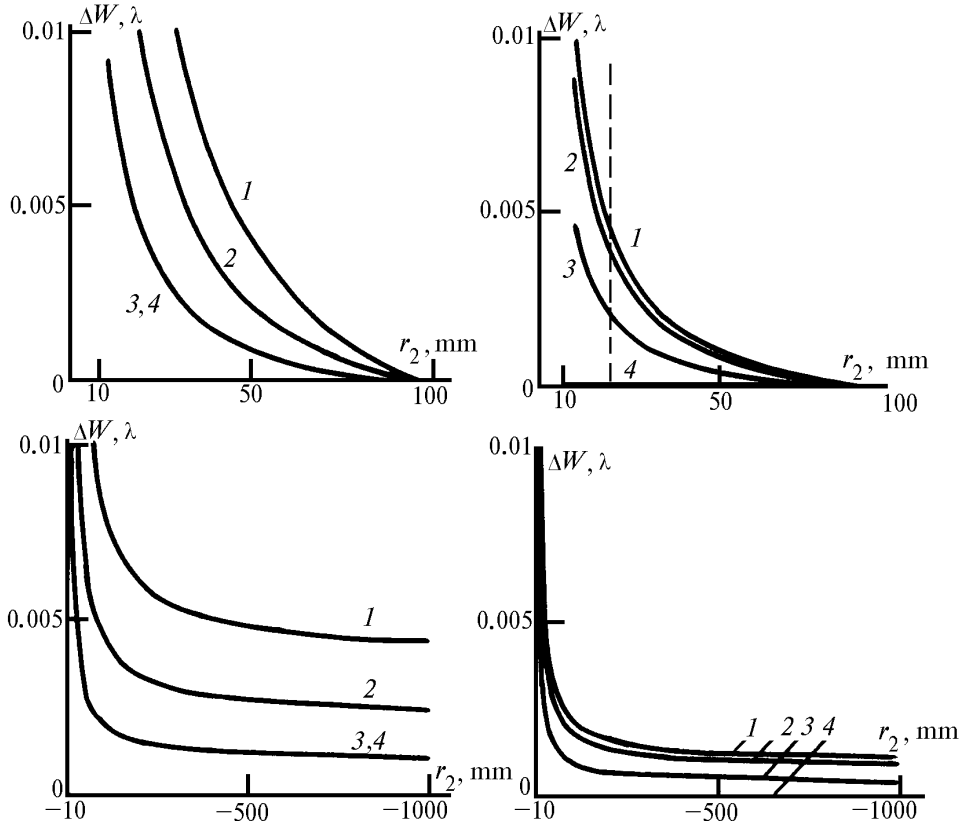

FIG. 4. Dependence of ΔW on the radius of the tested component for FI with $2a = 100$ mm, $R_r = 100$ mm, $W_{r.a.} = 2\lambda$. The curves correspond to: 1) spherical aberration; 2) coma; 3) astigmatism; 4) curvature of the image field; a, c) curvature center of the tested component in the Gaussian plane; b, d) in the plane of the best adjustment; a, b) for the convex surfaces; c, d) for the concave surfaces.

TABLE. Residual spherical aberration (μm) resulting in the error ΔW.

$2a$, mm	ΔW, wavelength	Relative apertures $2a/R_r$					
		1:0.66	1:1.5	1:3	1:10	1:50	1:70
30	1/500	0.511	0.403	0.296	0.163	0.072	0.061
	1/200	0.808	0.637	0.467	0.257	0.113	0.095
	1/100	1.141	0.898	0.658	0.362	0.158	0.132
	1/50	1.610	1.267	0.927	0.508	0.220	0.183
	1/20	2.535	1.991	1.454	0.790	0.336	0.279
100	1/500	0.935	0.738	0.542	0.300	0.133	0.196
	1/200	1.478	1.166	0.856	0.473	0.209	0.308
	1/100	2.088	1.647	1.209	0.667	0.294	0.434
	1/50	2.950	2.325	1.705	0.939	0.412	0.610
	1/20	4.653	3.663	2.683	1.472	0.640	0.952
150	1/500	1.446	0.904	0.664	0.367	0.307	0.354
	1/200	1.811	1.429	1.049	0.580	0.485	0.559
	1/100	2.559	2.018	1.482	0.818	0.684	0.789
	1/50	3.616	2.850	2.092	1.153	0.963	1.112
	1/20	5.706	4.494	3.294	1.811	1.511	1.746

The first two conclusions enable one to consider only the spherical aberration in the plane of the best adjustment, the third one makes it possible to restrict the investigated range of tested components. In other words, if the radius of a tested component satisfies the relation (6) at the light diameter $2a$ of the accessory lens *4* (Fig. 1), it is expedient to take another lens with the light diameter $2a' < 2a$ such that the relation (6) is not satisfied. Based on these assumptions, the results of the numerical experiment were represented in Table I. The light diameter $2a$ of the lens *4* (Fig. 1) and the relative aperture $2a/R_r$ of the standard sphere serve as parameters. Here, the restriction upon the length of the objective arm (6) and the relation

$$(R_r - R_{c.l.}) < 4000 \text{ mm}, \quad (7)$$

connected with the laser coherence length and vibration resistance demands were taken into account. The parameters $2a$ and $2a/R_r$ were chosen based on the analysis of existing industrial interferometers MARK-IV[8] and IKD-110.[9] Some violations in the dependence that follow from the Table can be explained by the inequality (7).

The results presented make possible to specify the maximum admissible value of aberrations $W_{r.a.}$ based on the ΔW value desired.

REFERENCES

1. D.T. Puryaev, *Test Methods for Optical Aspheric Surfaces* (Mashinostroenie, Moscow, 1976), 261 pp.
2. M.N. Sokol'skii, *Tolerance and Quality of Optical Image* (Mashinostroenie, Leningrad, 1986), 221 pp.
3. G.G. Slyusarev, *Methods of Calculating Optical Systems* (Mashinostroenie, Moscow, 1969), 652 pp.
4. M.A. Gan, S.I. Ustinova, and V.V. Kotov, Opt. Mekh. Promst., No. 8, 17 (1990).
5. I.G. Polovtsev and G.V. Simonova, Atm. Opt. **2**, No. 5, 456 (1989).
6. .G. Polovtsev and G.V. Simonova, Atm. Opt. **3**, No. 6, 605–610 (1990).
7. S.T. Kalinin, Opt. Mekh. Promst., No. 5, 16 (1991).
8. *MARK-IV XP. Interferometer System,* L.O.T. GMBH, Darmstadt.
9. *Catalog of LOMO Products* (St. Petersburg).